

# Diagnosis of gastric intestinal metaplasia with confocal laser endomicroscopy in vivo: a prospective study

## Authors

Y.-T. Guo<sup>1,2</sup>, Y.-Q. Li<sup>1</sup>, T. Yu<sup>1</sup>, T.-G. Zhang<sup>3</sup>, J.-N. Zhang<sup>1</sup>, H. Liu<sup>1</sup>, F.-G. Liu<sup>1</sup>, X.-J. Xie<sup>1</sup>, Q. Zhu<sup>1</sup>, Y.-A. Zhao<sup>1</sup>

## Institutions

<sup>1</sup> Department of Gastroenterology, Qilu Hospital, Shandong University, Jinan, China

<sup>2</sup> Department of Gastroenterology, the Second Affiliated Hospital, Shandong Traditional Medicine University, Jinan, China

<sup>3</sup> Department of Pathology, Qilu Hospital, Shandong University, Jinan, China

submitted 4 April 2007  
accepted after revision  
1 January 2008

## Bibliography

DOI 10.1055/s-2007-995633  
Published online: 2 April 2008  
Endoscopy 2008; 40:  
547–553 © Georg Thieme  
Verlag KG Stuttgart · New York  
ISSN 0013-726X

## Corresponding author

Y.-Q. Li, MD

Department of  
Gastroenterology  
Qilu Hospital, Shandong  
University  
Jinan 250012  
China  
Fax: +86-531-82169236  
liyanqing@sdu.edu.cn

**Background and study aims:** Gastric intestinal metaplasia (GIM) is a risk factor for development of intestinal-type gastric cancer. We aimed to assess the usefulness of confocal laser endomicroscopy (CLE) in diagnosing GIM.

**Patients and methods:** 28 patients with known GIM underwent CLE, and CLE criteria for diagnosis of GIM were developed. In addition, 53 consecutive patients with known or suspected GIM were prospectively evaluated.

**Results:** GIM was identified if any of the following three features were present in an image field: goblet cells, columnar absorptive cells and brush border, and villiform foveolar epithelium. GIM was then classified as complete or incomplete according to the shape of the goblet cells, the presence of absorptive cells or brush border, and the architecture of vessels and crypts. In a prospective study, a total of 13 670 CLE images were ob-

tained. Among 267 sites from 53 patients, 160 from 36 patients were diagnosed histopathologically as GIM. The sensitivities of conventional endoscopy and CLE for GIM were 36.88% vs. 98.13%, and the specificities were 91.59% vs. 95.33%, respectively. The kappa value for the correlation with histological findings was 0.25 for conventional endoscopy vs. 0.94 for CLE. The sensitivity and specificity of CLE were 68.03% and 89.66%, respectively, for the diagnosis of complete GIM, and 68.42% and 83.41%, respectively, for incomplete GIM; the kappa value for the correspondence between CLE and histological findings was 0.67.

**Conclusion:** CLE is a useful and potentially important method for the diagnosis and classification of GIM in vivo.

## Introduction

Gastric intestinal metaplasia (GIM) is a risk factor that leads to the development of intestinal-type gastric cancer [1]. The pathogenesis of GIM is probably a combination of factors related to both *Helicobacter pylori* and genetic aspects of the host; it is also likely that environmental factors are involved in this precancerous condition [2,3]. The diagnosis of GIM is based on histopathologic examination of endoscopic biopsy specimens.

Several previous studies have been carried out to develop up-to-date endoscopic criteria for diagnosing GIM [4–12]. Conventional endoscopic identification of GIM has a high rate of interobserver variability and correlates poorly with the histological findings [4]. Kaminishi et al. reported that conventional endoscopy was unsuitable for diagnosing intestinal metaplastic gastritis [5]. They found that macroscopic changes were specific (98%–99%), but not sensitive (6%–12%).

Chromoendoscopy with magnifying endoscopes and narrow-band imaging (NBI) techniques has been shown to improve the chance of diagnosis and analysis of GIM during endoscopy [6–12]. However, all of the above techniques are limited to the recognition of morphologic changes (mucosal and vascular patterns); biopsy and subsequent histological evaluation are still needed for the final diagnosis of GIM. None of them can distinguish the structure of individual cells, or allow the type of GIM to be defined. However, biopsy examinations require complex and time-consuming preparation procedures. This may limit the possibility for the endoscopist to make immediate diagnoses, resulting in the need for repeat endoscopic procedures. Furthermore, biopsies can lead to unnecessary risks for the patients.

Recently, a CLE has been developed which is integrated into the distal tip of a conventional video endoscope. The new device can provide real-time, high magnification, cross-sectional images

of the gastrointestinal epithelium during routine endoscopy. The greatest advantage of the microendoscope is its approximately 1000-fold magnification, which readily permits single cells in the gastrointestinal tract to be resolved.

The real-time, highly magnified images of the gastrointestinal tract mucosa can permit a histological diagnosis during endoscopy without the need for biopsy, and thus this technique has been termed “optical biopsy”. Several investigators have reported that the technique is of value [13–17], but as yet no studies have described its application in the classification of GIM. The aim of the present study was to clarify the diagnostic value of CLE for identifying and classifying GIM.

## Patients and methods



### Pilot study

A total of 28 patients with known GIM were recruited for a pilot study in the endoscopy unit of Shandong University's Qilu Hospital. The patients underwent CLE examinations in the manner described below. CLE images were evaluated and classified by three experienced endoscopists (Y.L., Y.Z., and T.Y.) and an experienced pathologist (T.Z.). The CLE images and corresponding histopathological images from normal and metaplastic areas were analyzed. The CLE features of GIM were identified by comparing the *in vivo* images and conventional *ex vivo* histopathology. Based on the histological diagnostic criteria for GIM [18], *in vivo* CLE criteria for diagnosing and classifying GIM were developed by the gastroenterologists and the pathologist. CLE images and biopsy samples of the duodenal mucosa were taken from five patients as references for intestinal mucosa.

### Prospective study

Between June 2006 and November 2006, 53 patients with GIM or suspected GIM were recruited into the prospective study. The inclusion criteria were: long-lasting upper gastrointestinal symptoms (>15 years), or atrophic gastritis or GIM identified at surveillance endoscopy. Patients meeting one or more of the following criteria were excluded from the study: presence of advanced adenocarcinoma in the stomach, acute gastrointestinal bleeding, coagulopathy, uncontrolled impaired renal or liver disease, pregnancy or lactation, allergy to fluorescein sodium, age younger than 18 years, and inability to provide written informed consent.

Informed written consent for participation in the study was obtained from each patient before the examination. The study protocol and consent forms were approved by the Human Subjects Committee and Ethics Committee of Shandong University's Qilu Hospital.

### Endoscopic procedures

All patients were prepared for routine gastroscopy, and scopolamine butylbromide 20 mg (Yantai Luyin Pharmaceutical Co., China) was then given before endoscopy.

First, all of the stomach was visualized using standard white light. After routine observation, standard positions were carefully examined using the CLE system (Pentax EC-3870K; Pentax, Tokyo, Japan). These areas included two from the gastric antrum and two from the gastric body [18]. Areas of abnormal appearance were also examined with the confocal laser imaging system. These visible lesions included areas of whitish color change

with plaques, patches, or homogeneous discoloration on the gastric mucosa [19].

For the CLE procedure, in all patients fluorescein sodium (5–10 ml of 10% solution; Guoangzhou Baiyunshan Mingxing Pharmaceutical Co. Ltd, China) was intravenously administered during endoscopy. The site of interest was placed at the lower left corner of the CLE window, and the distal tip of the endoscope was placed in gentle contact with the mucosa using blue laser as guide. The position of the focal plane within the specimen was adjusted using the buttons on the endoscope control panel. We applied suction to maintain a stable position. The “optical biopsy” site was located 5 mm immediately to the left of the “polyp” created by suction. Every site of interest in the mucosal layer could be scanned from the surface to the deeper areas, and images could be captured by operating a foot pedal. Areas were rinsed with water if details were obscured by mucus. Afterwards, a targeted biopsy was done at the same sites.

The CLE procedures were done by three experienced endoscopists (Y.L., Y.Z., and T.Y.), who had all carried out more than five CLE procedures before the beginning of our study. A conventional endoscopic diagnosis and a preliminary CLE diagnosis regarding GIM were made immediately by the endoscopist at the time of the procedure.

The CLE images can be stored as digital files, and all the digitally stored images within a specific area were reassessed for accuracy and quality by an experienced investigator who was blinded to the patients' endoscopic findings (Y.G.). The final CLE diagnosis regarding GIM was made on the basis of the newly developed criteria. GIMs were further classified as complete or incomplete types by the investigator.

In addition, the quality of every CLE image was scored as good (no moving artifacts, single cells could be delineated), average (artifacts present but tissue structure could be recognized), or poor (artifacts did not allow recognition of the image) [13]. The endoscopic diagnoses for the different areas were compared with the histological features of biopsy specimens.

### Histological assessment

All the biopsy specimens were immersed in formalin, embedded in paraffin and sectioned vertically and transversely to facilitate the comparison between histopathologic and CLE images. Afterwards, the serial sections (4- $\mu$ m) were stained with hematoxylin and eosin for histopathological examination.

All biopsy specimens were reviewed by an experienced pathologist blinded to the CLE results. To assess the diagnostic accuracy, GIM was regarded as being present histologically when at least a single goblet cell was seen in sections of the biopsy. Patients were diagnosed as GIM-positive if GIM was present in at least one of the biopsy specimens. GIMs were classified as complete (type I) and incomplete (type II or III) based on morphology and mucin staining [18,20,21], with AB-PAS and HID-AB mucin staining being applied in parallel sections for this purpose.

### Statistical analysis

The sensitivity, specificity, and positive and negative predictive values of the CLE patterns for the detection of GIM were calculated. To further assess the level of agreement between endoscopic images and histopathology, kappa values were calculated, with 95% confidence intervals. Agreement was regarded as poor with values below 0.4, good with values between 0.4 and 0.75, and excellent with values over 0.75. Only values greater than 0.4 were considered good enough for diagnostic reliability. Con-

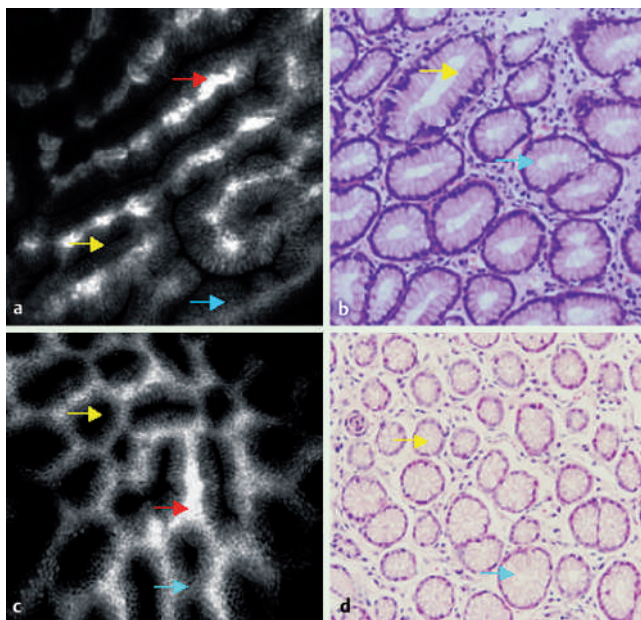


**Fig. 1** CLE and corresponding histological images of normal gastric mucosa. **a** The CLE image of gastric antrum shows longitudinal glandular openings (yellow arrow). Columnar mucus cells (blue arrow) and the regular subepithelial capillary network (red arrow) are easily identified. **b** Corresponding histological appearance of gastric antrum. **c** The CLE image from the gastric body shows round or oval glandular openings (yellow arrow). Columnar mucus cells (blue arrow) and a regular subepithelial capillary network (red arrow) are also present. **d** Corresponding histological specimen of gastric body.

confidence intervals were calculated only for statistically significant values. A chi-squared analysis was done for comparisons. A *P* value of less than 0.05 was considered to be statistically significant.

## Results

### Pilot study: CLE findings

Fluorescein sodium was distributed throughout the entire mucosa from less than 20 s after the intravenous injection to 20 minutes afterwards. The nuclei of epithelial cells could not be visualized with fluorescein as contrast agent (▶ **Fig. 1**). The

glandular openings of the foveolae gastricae had a rather longitudinal shape at the antrum (**Fig. 1 a**) and were approximately round or oval-shaped at the cardia or body (▶ **Fig. 1 c**). The regular submucosal microvasculature contained within the stroma could be identified easily. CLE images corresponded well with the appearances of the hematoxylin-eosin stained transverse sections of the biopsy specimens from the same sites (▶ **Fig. 1 b, d**).

Based on correspondence with histopathological appearances, goblet cells, villiform foveolar epithelium, and columnar absorptive cells and brush borders could be easily identified in CLE images (▶ **Fig. 2–4**). The duodenal villi, goblet cells, and absorptive cells with brush border could also be delineated in the CLE images of the duodenal mucosa (▶ **Fig. 3 g–i**). Thus GIM was identified if any of the three following three features was present in an image field:

- ▶ Goblet cells (▶ **Fig. 2–4**): large black cells with mucin contrast to surrounding columnar-lined epithelium cells.
- ▶ Villiform shape of foveolar epithelium (▶ **Fig. 3 a, d, Fig. 4 a**): a typical villous-like appearance different from the antral or corpus foveolae gastricae.
- ▶ Columnar absorptive cells (▶ **Fig. 2–4**) and brush border (▶ **Fig. 3 d**): more slender, and brighter than columnar mucus cells of normal gastric mucosa, with a clear dark line at the surface of the epithelium.

In the CLE images, GIM was further classified as complete or incomplete (▶ **Fig. 4**), according to the shape of goblet cells [22], the presence of absorptive cells or brush border, and the architecture of vessels and crypts [13, 14], as follows:

- ▶ Complete: goblet cells interspersed among absorptive cells with or without brush borders; with regular crypts and capillaries.
- ▶ Incomplete: smaller numbers of goblet cells scattered among gastric-type cells (mucus cells); without absorptive cells and brush border; with tortuous and branched crypts or irregular capillaries [13].

### Prospective study: CLE findings

A total of 53 patients (38 men, 15 women; median age 51.2 years, range 34–79) met all inclusion criteria and were enrolled in the study between June and November 2006. Participation in the study, which included upper endoscopy and CLE, was complete for all patients. The clinical characteristics of the patients who underwent CLE are shown in ▶ **Table 1**.

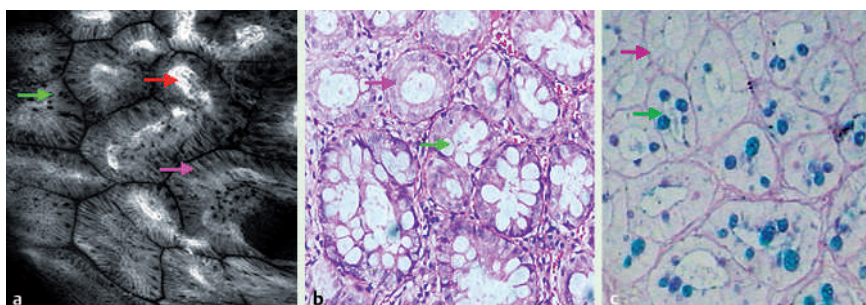


**Fig. 2** CLE images and corresponding histological images of GIM from mucosa of the gastric body.

**a** The CLE image following intravenous administration of fluorescein shows strong staining of the surface epithelium as well as the regular subepithelial capillary network (red arrow). Goblet cells (green arrow) are large and very dark within the columnar epithelium (purple ar-

row). **b** Corresponding histological appearance of GIM of the mucosa. **c** The histological appearance with AB-PAS mucin staining showed goblet cells (green arrow) and columnar epithelium (purple arrow, corresponding to absorptive cells).

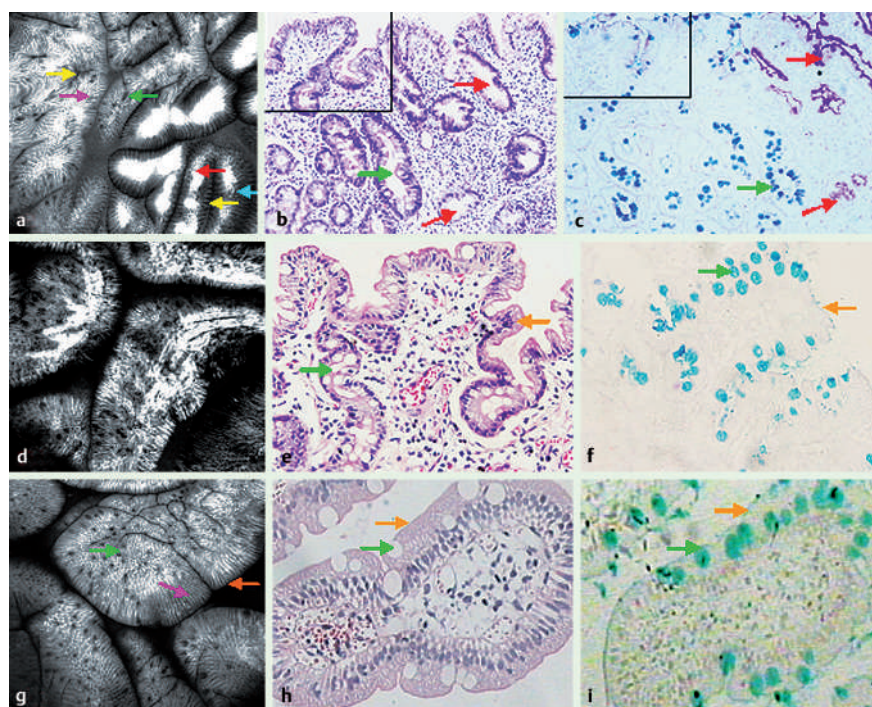


**Fig. 3** Features of GIM in CLE images.

**a** The CLE image obtained from the gastric antrum shows the borderline between metaplasia (top left) and normal area (low right). Typical villous-like foveolar epithelium and goblet cells (green arrow) can be seen in metaplastic areas. Columnar absorptive cells (purple arrow) were more slender and brighter than columnar mucus cells (blue arrow). Yellow arrows show the glandular openings. **b** Histological image corresponding to **Fig. 3 a** shows the mucosa with GIM (green arrow) and normal gastric mucosa (red arrow). **c** Histological appearance with AB–PAS mucin staining shows the GIM (green arrow) and normal gastric mucosa (red arrow). Goblet cells are stained blue and absorptive cells are colorless; gastric columnar mucus cells are stained purple. **d** CLE image of typical villous-like foveolar epithelium of

GIM. **e** Histological appearance of **Fig. 3 d** at higher magnification. Goblet cells (green arrow) and brush border (orange arrow) can be identified. **f** Histological appearance of **Fig. 3 e** at higher magnification. Goblet cells (green arrow) and brush border (orange arrow) can be identified. **g** CLE image of duodenal mucosa. The villous-like structure, goblet cells (green arrow), columnar absorptive cells (purple arrow) and brush border (orange arrow) can be identified. **h** Corresponding histological image of duodenal mucosa with goblet cells (green arrow) and brush border (orange arrow). **i** The histological image with HID–AB mucin staining. Goblet cells are stained green and absorptive cells are colorless.

A total of 13 670 CLE images, from 267 different sites in 53 patients were obtained. Regarding image quality, 4920 (36%) were good, 4510 (33%) were average, and the remainder were poor. GIM was finally identified in 162 sites from 36 patients on the basis of the CLE criteria.

The mean duration of the examination was 20 minutes (range 12–32).

#### Overall accuracy of CLE for diagnosing GIM

The complete data comparing the diagnosis of GIM by endoscopy, at preliminary assessment with CLE, at final CLE assessment, and by histopathology are summarized in **Tables 2** and **3**.

A total of 267 sites from 53 patients were sampled. Of the 267 biopsy specimens, 160 from 36 patients were diagnosed histopathologically as GIM.

At endoscopy, a total of 68 sites of abnormal appearance were diagnosed as GIM; of these, 59 were identified as GIM-positive and 9 as GIM-negative by CLE, and this diagnosis was confirmed by histopathology. Of the 199 sites that appeared normal at conventional endoscopy, 103 of them were diagnosed as GIM by CLE, with 101 of these being confirmed by histopathology. The sensitivity, specificity, positive predictive value and negative predictive value of conventional endoscopy for the diagnosis of GIM were 36.88%, 91.59%, 86.76% and 49.25%, respectively. The kappa score for the agreement between conventional endoscopy and histopathology was only 0.25.

CLE proved to be significantly superior to conventional endoscopy. A total of 162 sites were finally diagnosed ultimately as having GIM by CLE, with 157 of them being identified as GIM-positive by histopathology and 5 of them as GIM-negative. Of the 105 sites diagnosed GIM-negative by CLE, this was confirmed by histopathology in 102 of them. This comparison showed that GIM could be predicted by CLE with a sensitivity of 98.13%, a specificity of 95.33%, a positive predictive value of 96.91%, and a negative predictive value of 97.14%. The kappa score for the correlation between CLE and histopathology was 0.94 (95% CI 0.82–1.00). The final CLE diagnosis of GIM tended to be more accurate than the preliminary one, but this was not statistically significant ( $P=0.1456$ ).

#### Accuracy of CLE for classifying GIM

The agreement between the CLE and histological diagnoses for type of GIM is shown in **Table 4**. With regard to type, the CLE findings corresponded to the histopathology results. Of the 26 sites, 102 were uniformly diagnosed GIM negative, 83 were complete GIM and 26 were incomplete GIM by histopathology and CLE.

Among the 98 sites with complete GIM according to CLE, this was confirmed in 83 by histopathology. The sensitivity, specificity, positive predictive value and negative predictive value of CLE for the diagnosis of complete GIM were 68.03%, 89.66%, 84.69% and 76.92%, respectively.

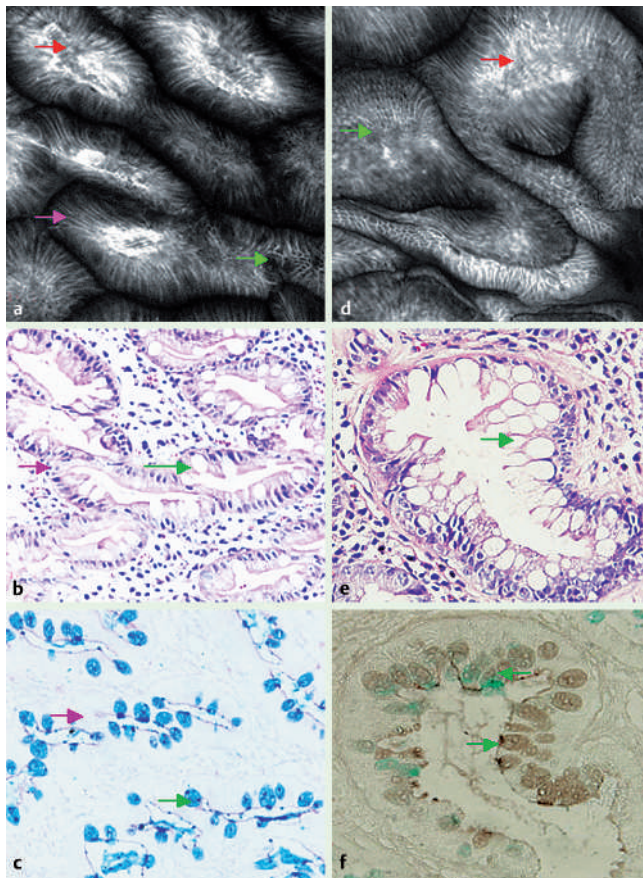


**Fig. 4** CLE images and corresponding histological images of complete and incomplete GIM from gastric antrum. **a** CLE appearance of complete GIM. The red arrow shows the villous-like foveolar epithelium with regularly shaped capillaries. Goblet cells (green arrow) and absorptive cells (purple arrow) can be seen. **b** Corresponding histological image of complete GIM with regular glands, goblet cells (green arrow) and columnar mucus cells (purple arrow). **c** Corresponding histological image with AB-PAS mucin staining. Goblet cells (green arrow) are stained blue and columnar cells are colorless (purple arrow, corresponding to absorptive cells). **d** CLE appearance of incomplete GIM obtained from the antrum. Goblet cells (green arrow) can be seen with tortuous foveolae and irregular capillaries (red arrow). **e** Corresponding histological image of incomplete GIM. Small and less numerous goblet cell vacuoles (green arrow) with irregular glands can be seen. **f** Corresponding histological image with HID-AB mucin staining. Most goblet cells are stained brown with a small number of goblet cells green. Some columnar cells were stained brown.

Among the 64 sites with incomplete GIM according to CLE, this was confirmed histologically in 26. The sensitivity, specificity, positive predictive value and negative predictive value of CLE for the diagnosis of incomplete GIM were 68.42%, 83.41%, 40.63% and 94.09%, respectively. The kappa score for the agreement between CLE and histopathology was 0.67 (95% CI 0.59–0.76).

## Discussion

GIM is defined as replacement of glandular and/or foveolar epithelium by intestinal epithelium [18]. Epidemiological studies have shown that GIM in the stomach has a high cancer risk and is therefore defined as a precancerous condition [23]. Metaplastic epithelium can be recognized morphologically by the pres-

Patients, n	53
Mean age (range), years	51 (34–79)
Sex, n (%)	
Male	38 (72)
Female	15 (28)
Intestinal metaplasia, n (%)	
Present	36 (68)
Absent	17 (32)

**Table 1**  
Clinical characteristics of patients undergoing CLE

ence of goblet cells, absorptive cells, Paneth cells and villous-like foveolar epithelium, or by its enzyme or mucin content. The results of the present study showed that these cells and architecture can be identified in images provided by CLE.

The key endoscopic findings for diagnosing GIM are based on the abnormal appearance of the mucosa [19]. In the present study, the diagnostic sensitivity and specificity obtained from conventional endoscopy was equal to that previously reported [4,5]. The kappa score for the correspondence between endoscopy and histopathology was 0.25, indicating a poor agreement for diagnostic reliability.

In contrast to conventional endoscopy, in the present study endoscopy with CLE provided images of cells and subcell structures, such as goblet cells, absorptive cells, villous-like foveolar epithelium and brush border. Thus, with this endoscopic modality the diagnostic criteria for GIM were same as the histopathologic criteria. Goblet cells are the most frequent and typical feature of GIM. All of the 160 sites of GIM diagnosed by histopathology had goblet cells in the corresponding CLE images. Goblet cells displayed distinctive features in CLE images and were easily identified; as fluorescein cannot stain mucins strongly, the mucins in the goblet cells are darker than surrounding structures. In CLE images, columnar absorptive cells appeared more slender and brighter than mucus cells of normal gastric mucosa at the surface of the epithelium. It may be speculated that the appearance is caused by different tissue fluorescence characteristics or by the distribution of fluorescein at the surface of the ciliated tissue structure. Due to the presence of absorptive cells, the foveolar epithelium has a typical villous-like shape in metaplastic areas; these villous-like patterns have also been seen at NBI in patients with GIM [6]. Unlike the other features of GIM, the brush border was seldom seen in the CLE images, as the brush border is the superficial microvilli of absorptive cells and can be seen only when glands are longitudinally sectioned. Similar features regarding cells and architecture were also observed in the duodenal mucosa, where the duodenal villi, goblet cells, and absorptive cells with brush border were delineated.

In the present study, CLE images of GIM corresponded well with histopathological images. By directly comparing the results from in vivo laser endomicroscopy and subsequent histopathological examination of biopsy specimens, we observed that CLE could diagnose the presence of GIM with high accuracy. For the diagnosis of GIM, the sensitivity was 98.13%, the specificity was 95.33%, and the positive and negative predictive values were 96.91% and 97.14% respectively. The statistical results demonstrate that this newly developed optical technology can provide endoscopic visualization of regions of GIM in the gastrointestinal tract without the need for biopsy.

In our study, due to the speed at which the CLE images were scanned during endoscopy, a few goblet cells and other details were not identified by the endoscopist. The preliminary CLE diagnosis was less accurate. Hence these CLE images were later reassessed blindly by an experienced investigator for a final CLE

**Table 2** Comparison of conventional endoscopy, CLE, and histopathology for diagnosing GIM at 267 sites

		Endoscopy		Preliminary CLE		Final CLE	
		GIM (+)	GIM (-)	GIM(+)	GIM(-)	GIM(+)	GIM(-)
<b>Histopathology</b>							
GIM (+)	160	59	101	146	14	157	3
GIM (-)	107	9	98	9	98	5	102
Total	267	68	199	155	112	162	105

	Endoscopy	Preliminary CLE	Final CLE
Sensitivity, %	36.88	91.25	98.13
Specificity, %	91.59	91.19	95.33
PPV, %	86.76	94.19	96.91
NPV, %	49.25	87.50	97.14
Kappa coefficient (95% CI)	0.25	0.82 (0.70–0.94)	0.94 (0.82–1.00)

PPV, positive predictive value; NPV, negative predictive value.

**Table 3** Conventional endoscopy and CLE in the diagnosis of GIM

	Total, n	Histological diagnosis, n		
		None	Complete	Incomplete
<b>CLE diagnosis</b>				
None	105	102	1	2
Complete	98	5	83	10
Incomplete	64	0	38	26

**Table 4** Correspondence between CLE and histopathology for diagnosing the subtype of GIM at 267 sites

diagnosis regarding GIM. Therefore, we have two sets of values for diagnostic discrimination, one developed from live CLE images assessed contemporaneously and without blinding, and a final one derived from blind assessment. We found that the final CLE diagnosis for GIM tended to be more accurate than the preliminary one, but this was not statistically significant ( $P=0.1456$ ).

GIMs have been classified as complete (type I) and incomplete (type II or III) [20,21], and complete metaplasia is believed to carry the lower risk of gastric cancer, whereas incomplete forms of metaplasia have been closely linked to carcinoma [24,25]. Most GIMs are only “precancerous conditions” rather than “precancerous lesions” [26]. These studies confirmed that classifying GIM is essential, in order to assess the risk of gastric cancer and provide appropriate follow-up for patients with GIM [27]. In the present study, the GIM subtype could be defined using CLE. The kappa score for the correspondence between CLE and histopathology for the diagnosis of the subtype of GIM was 0.67, indicating a good agreement for diagnostic reliability. These results confirm a previous study that GIM can be categorized into complete and incomplete forms on the basis of morphology [22]; the authors classified the GIM subtype according to the architectural derangement, and the mature absorptive and goblet cells. It is difficult to recognize absorptive cells in hematoxylin and eosin (H&E)-stained sections, and they are often identified with the help of mucin staining. In the present study, architectural derangement and absorptive cells and goblet cells could be easily identified using CLE. In addition, capillaries of irregular shape are also indicators of incomplete GIM. CLE can show high resolution images of capillaries filled with erythrocytes. The results of our study indicated that irregular capillaries were more often associated with incomplete GIM.

Nevertheless in the present study CLE did not distinguish very well between incomplete and complete GIM, with sensitivities

for the diagnosis of complete and incomplete GIM of only 68.03% and 68.42%, respectively. This is because of the properties of the CLE system. First, the surface area examined at CLE is very small ( $475 \times 475 \mu\text{m}$ ), which would make it time-consuming to investigate the entire surface area from which the corresponding biopsy is taken. Also, the tip of the endoscope could not be specifically targeted to the lesion. Secondly, the penetration depth of blue laser light is limited to only the upper part of the mucosal layer ( $250 \mu\text{m}$ ). Therefore, the diagnosis of GIM and subtype was based on the upper part of the crypt rather than the whole crypt. Interestingly though, a previous study has shown good correlation between the GIM in the upper and lower parts of crypts [22]. Thirdly, the diagnostic accuracy was also influenced by the quality of the CLE images. With the development of technique and operating skill, this problem of discrimination between incomplete and complete GIM can be overcome.

In conclusion, our results showed that CLE, the newly developed method for studying GIM, may offer virtual in vivo histological observation of the mucosal layer. It is very useful for the diagnosis and classification of GIM. Furthermore, CLE can not only detect with high accuracy the presence of GIM, but can also efficiently follow up the patient's metaplastic condition. However, currently this modality might not be sufficient to replace histological examination. These preliminary findings are based on a small number of patients and to confirm these results a larger number of such patients should be evaluated. In addition, the results need to be validated at different centers, and the inter- and intraobserver variability must be tested. We believe that, with development and improvement of this technique, CLE will be used for the diagnosis of gastric lesions and will have important clinical implications in the future.

**Competing interests:** None

## References

- 1 Walker MM. Is intestinal metaplasia of the stomach reversible? *Gut* 2003; 52: 1–4
- 2 Zhou L, Sung JJ, Lin S *et al.* A five-year follow-up study on the pathological changes of gastric mucosa after *H. pylori* eradication. *Chin Med J (Engl)* 2003; 116: 11–14
- 3 Kato I, Vivas J, Plummer M *et al.* Environmental factors in *Helicobacter pylori*-related gastric precancerous lesions in Venezuela. *Cancer Epidemiol Biomarkers Prev* 2004; 13: 468–476
- 4 Sauerbruch T, Schreiber MA, Schüssler P *et al.* Endoscopy in the diagnosis of gastritis: diagnostic value of endoscopic criteria in relation to histological diagnosis. *Endoscopy* 1984; 16: 101–104
- 5 Kaminishi M, Yamaguchi H, Nomura S *et al.* Endoscopic classification of chronic gastritis based on a pilot study by the Research Society for Gastritis. *Dig Endosc* 2002; 14: 138–151
- 6 Uedo N, Ishihara R, Iishi H *et al.* A new method of diagnosing gastric intestinal metaplasia: narrow-band imaging with magnifying endoscopy. *Endoscopy* 2006; 38: 819–824
- 7 Dinis-Ribeiro DM, da Costa-Pereira C, Lopes C *et al.* Magnification chromoendoscopy for the diagnosis of gastric intestinal metaplasia and dysplasia. *Gastrointest Endosc* 2003; 57: 498–504
- 8 Kim S, Harum K, Ito M *et al.* Magnifying gastroendoscopy for diagnosis of histologic gastritis in the gastric antrum. *Dig Liver Dis* 2004; 36: 286–291
- 9 Gheorgh C. Narrow-band imaging endoscopy for diagnosis of malignant and premalignant gastrointestinal lesions. *J Gastrointest Liver Dis* 2006; 15: 77–82
- 10 Nakayoshi T, Tajiri H, Matsuda K *et al.* Magnifying endoscopy combined with narrow band imaging system for early gastric cancer: correlation of vascular pattern with histopathology (including video). *Endoscopy* 2004; 36: 1080–1084
- 11 Kara MA, Ennahachi M, Fockens P *et al.* Detection and classification of the mucosal and vascular patterns (mucosal morphology) in Barrett's esophagus by using narrow band imaging. *Gastrointest Endosc* 2006; 64: 155–166
- 12 Ydgi K, Honda H, Yang JM *et al.* Magnifying endoscopy in gastritis of the corpus. *Endoscopy* 2005; 37: 660–666
- 13 Kiesslich R, Gossner L, Goetz M *et al.* In vivo histology of Barrett's esophagus and associated neoplasia by confocal laser endomicroscopy. *Clin Gastroenterol Hepatol* 2006; 4: 979–987
- 14 Kiesslich R, Burg J, Vieth M *et al.* Confocal laser endoscopy for diagnosing intraepithelial neoplasias and colorectal cancer in vivo. *Gastroenterology* 2004; 127: 706–713
- 15 Kiesslich R, Goetz M, Burg J, Stolte M *et al.* Diagnosing *Helicobacter pylori* in vivo by confocal laser endoscopy. *Gastroenterology* 2005; 128: 2119–2123
- 16 Kakeji Y, Yamaguchi S, Yoshida D *et al.* Development and assessment of morphologic criteria for diagnosing gastric cancer using confocal endomicroscopy: an ex vivo and in vivo study. *Endoscopy* 2006; 38: 886–890
- 17 Kitabatake S, Niwa Y, Miyahara R *et al.* Confocal endomicroscopy for the diagnosis of gastric cancer in vivo. *Endoscopy* 2006; 38: 1110–1114
- 18 Dixon MF, Genta RM, Yardley JH *et al.* Classification and grading of gastritis. The updated Sydney System. International Workshop on the Histopathology of Gastritis, Houston 1994. *Am J Surg Pathol* 1996; 20: 1161–1181
- 19 Lin BR, Shun CT, Wang TH *et al.* Endoscopic diagnosis of intestinal metaplasia of stomach – accuracy judged by histology. *Hepatogastroenterology* 1999; 46: 62–166
- 20 Sipponen P, Kosunen TU, Valle J *et al.* *Helicobacter pylori* infection and chronic gastritis in gastric cancer. *J Clin Pathol* 1992; 45: 19–323
- 21 Filipe MI, Munoz N, Matko I *et al.* Intestinal metaplasia types and the risk of gastric cancer: a cohort study in Slovenia. *Int J Cancer* 1994; 57: 324–329
- 22 Tosi P, Filipe MI, Baak JP *et al.* Morphometric definition and grading of gastric intestinal metaplasia. *J Pathol* 1990; 161: 201–208
- 23 You WC, Zhang L, Gail MH *et al.* Precancerous lesions in two counties of China with contrasting gastric cancer risk. *Int J Epidemiol* 1998; 27: 945–948
- 24 Tosi P, Filipe MI, Luzzi P *et al.* Gastric intestinal metaplasia type III cases are classified as low-grade dysplasia on the basis of morphometry. *J Pathol* 1993; 169: 73–78
- 25 Meining A, Morgner A, Miehle S *et al.* Atrophy–metaplasia–dysplasia–carcinoma sequence in the stomach: a reality or merely an hypothesis? *Best Pract Res Clin Gastroenterol* 2001; 15: 983–998
- 26 Rokkas T, Filipe MI, Sladen GE. Detection of an increased incidence of early gastric cancer in patients with intestinal metaplasia type III who are closely followed up. *Gut* 1991; 32: 1110–1113
- 27 Dinis-Ribeiro M, Lopes C, da Costa-Pereira A *et al.* A follow up model for patients with atrophic chronic gastritis and intestinal metaplasia. *J Clin Pathol* 2004; 57: 177–182